AIAA JOURNAL
Vol. 32, No. 1, January 1994

Validity of Linearized Unsteady Euler Equations with Shock Capturing

Dana R. Lindquist* and Michael B. Giles†
Massachusetts Institute of Technology, Cambridge, Massachusetts 02139

By examining the nature of shock movement, this article first shows that the unsteady lift due to the movement of a shock is linear with the magnitude of the shock movement. The argument that is presented holds true regardless of the shock structure, which is determined by the level of viscosity. This proof is the basis for showing that the linear perturbation equations can be used to determine not only the unsteadiness of the flowfield away from the shock but also the effect of the shock movement as well. Shock capturing is a computational technique that in effect adds a large amount of viscosity in the shock region, smearing shocks over several cells. After proving that the analytical linear viscous equations can be used to represent the flowfield, computational aspects relating to shock capturing are examined. These arguments provide the basis for using the linearized unsteady Euler equations with shock capturing as a viable computational technique. The strength of this new technique is the reduced computational effort required to find the effect of an unsteady perturbation on the flowfield.

Introduction

UNSTEADY flow calculations are of great importance to the aeronautical gas turbine industry because of the need to predict the onset of flutter, as well as the magnitude of forced response loading and oscillations. In recent years, many methods have been developed to solve the unsteady, nonlinear, two-dimensional and three-dimensional Euler or Navier-Stokes equations, but these methods are in general too expensive for everyday industrial use. Therefore, industry continues to use two-dimensional, linearized potential methods that require significantly less computational effort for most unsteady calculations.[1,2] These methods are limited, however, in their suitability for flows with moderate shocks and three-dimensional vorticity. Accordingly, there is a strong interest in developing a new class of methods, linearized Euler methods, in which the steady and unsteady flows can be both three-dimensional and vortical and the only assumption is that the level of unsteadiness is small.[3-7]

A two-dimensional linearized Euler method was developed by Hall and Crawley[3] and Hall,[8] who showed the usefulness of the linear assumption up to surprisingly large levels of unsteadiness. This work also demonstrated a limited capacity for shock fitting. This is an important subject because a significant fraction of the unsteady lift in compressor or fan flutter comes from the shock motion.

It is believed, however, that shock fitting in three dimensions will prove to be an intractable problem, and so an alternative shock-capturing approach has been developed. Although Whitehead[1] and Verdon and Casper[2] have used linearized shock capturing with the potential equations, their work lacks any mathematically rigorous justification. The purpose of this paper is to prove the validity of using shock capturing in perturbation methods. This proof is based on the linearization of the standard, unsteady, nonlinear shock-capturing Euler methods and will be used to define a new perturbation scheme.

Presented as Paper 91-1598 at the AIAA 10th Computational Fluid Dynamics Conference, Honolulu, HI, June 24-26, 1991; received March 30, 1992; revision received June 5, 1993; accepted for publication June 27, 1993.

*Research Assistant; currently Manager of Customer Services, Flomerics Inc., 57 East Main Street, Suite 201, Westborough, MA 01581.

†Associate Professor; currently Rolls-Royce Reader in Computational Fluid Dynamics, 11 Keble Rd., Oxford, England, UK. Member AIAA.

Analysis of the Navier-Stokes Equations

There are discretization and computational issues associated with modeling an unsteady transonic flowfield, but before considering these issues a better understanding of the analytical problem must be gained. In particular, the interest is in shock motion. Since viscosity plays an important role in the detailed characteristics of a shock, the analysis will start with the Navier-Stokes equations. The first flowfield that will be examined is a constant area duct since this represents the simplest transonic flowfield. Next, a variable area duct, which has a gradient in the flow upstream and downstream of the shock, will be studied to more realistically represent two- and three-dimensional flowfields.

Shock Motion in a Constant Area Duct

A moving shock in a constant area duct is usually referred to experimentally as a shock tube and is often used to probe the internal structure of a shock. Here it will be used to isolate and explore the effect of viscosity on a moving shock. An understanding of the analytical solution to the shock tube problem will point to features of the flowfield that must be modeled computationally.

Since the effect of viscosity is of interest, the one-dimensional Navier-Stokes equations will be considered:

$$\frac{\partial U}{\partial t} + \frac{\partial F_E}{\partial x} + \frac{\partial F_V}{\partial x} = 0 \tag{1}$$

where

$$U = \begin{bmatrix} \rho \\ \rho u \\ \rho E \end{bmatrix}, \quad F_E = \begin{bmatrix} \rho u \\ \rho u^2 + p \\ \rho u H \end{bmatrix}, \quad F_V = \begin{bmatrix} 0 \\ -\tau_{xx} \\ u\tau_{xx} - q_x \end{bmatrix} \tag{2}$$

In the previous expression for the viscous flux F_V, τ_{xx} is the viscous stress with viscosity μ and q_x is the heat conduction term with conductivity κ,

$$\tau_{xx} = \mu \frac{\partial u}{\partial x}$$

$$q_x = -\kappa \frac{\partial T}{\partial x}$$

which both cause the viscous term to be the second derivative of a flow variable.

The steady solution lends insight to the unsteady problem; therefore it will be looked at first. Integrating the steady form of Eq. (1) from one end of the duct to the other gives

$$\begin{aligned} F_E + F_V &= (F_E + F_V)_{\text{upstream}} \\ &= (F_E + F_V)_{\text{downstream}} \\ &= \text{const} \end{aligned} \tag{3}$$

For a given constant of integration, it is possible to have a solution where the upstream and downstream states are different and still satisfy Eq. (3), as well as the obvious trivial solution where the states are the same. Here the more complicated and interesting case where the states are different is considered. A final assumption is that the gradients at the upstream and downstream boundaries will be zero, and so in the boundary regions of the duct the trivial solution holds:

$$\left(\frac{\partial U}{\partial x}\right)_{\text{upstream}} = \left(\frac{\partial U}{\partial x}\right)_{\text{downstream}} = 0 \tag{4}$$

By assuming the gradients are zero, one finds that the viscous flux F_V in these regions of the duct is also zero. Since the constant in Eq. (3) that governs the flowfield is now only a function of the Euler fluxes, the magnitude of the viscosity does not govern the nature of the flowfield. What this provides is a flowfield where the solution near the boundaries is inviscid and the viscous region is restricted to the interior of the flowfield. Now, if the equations are rescaled by creating a new variable $\xi = x/\mu_{\text{ref}}$, where μ_{ref} is some reference viscosity, the equation in ξ no longer has a dependence on the viscosity μ but only on a nondimensionalized viscosity μ/μ_{ref}, which further says that the role of the viscosity is only to scale the viscous region. The role of the conductivity κ is similar to that of the viscosity and now becomes the scaled quantity κ/μ_{ref}. Since the role of the conductivity is similar to the role of the viscosity, future references to the viscosity will likewise hold for the conductivity. An inviscid, or Euler, solution can be found by taking the limit $\mu/\mu_{\text{ref}} \to 0$. In this Euler flowfield the flows upstream and downstream are constant and invariant along the duct, and so the only possibility is that the two regions are joined by a true discontinuity. The role of the viscosity is merely to provide a smooth form of this discontinuity, and it is the actual level of the viscosity that determines how wide this region is. From Eq. (3) it can be seen that the jump across the discontinuity, which is called a shock, is given by

$$(F_E)_{\text{upstream}} = (F_E)_{\text{downstream}} \tag{5}$$

which can be rewritten in a shorthand notation as

$$[\![F_E]\!] = 0 \tag{6}$$

where $[\![\cdot]\!]$ means the jump across the shock. Some computational schemes use these jump conditions as an internal boundary condition in the flowfield and model the shock as a true discontinuity; this is referred to as shock fitting.

Since in the steady case the viscosity only plays a role in stretching the shock region and not in determining the flowfield away from the shock, the level of viscosity can be changed and the overall nature of the solution remains the same. Computationally, this means the shock region can be modeled with an artificial viscosity that only needs to model the nature of the true viscous terms. This is helpful since the true viscosity would produce shocks with widths of molecular scales that cannot be represented on a larger computational grid where shocks with widths of a few computational cells are desired.

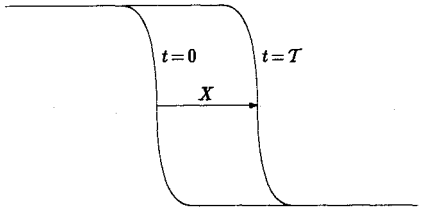

Fig. 1 Displacement of a shock in an unsteady shock tube.

But the analysis presented thus far is only for a stationary shock. What happens if the shock moves? Does the level of the viscosity again only play the role of scaling the width of the shock region? These are important questions that must be addressed when considering unsteady flowfields. Again, to model the flowfield computationally, the role of the viscosity must be known. It would be nice to be able to use the artificial viscosity model for unsteady flowfields as well as steady flowfields.

Equation (1) is again integrated along the duct, but now the unsteady term is retained in the equation:

$$\frac{\mathrm{d}}{\mathrm{d}t}\int U\,\mathrm{d}x + (F_E + F_V)_{\text{downstream}} - (F_E + F_V)_{\text{upstream}} = 0 \tag{7}$$

Once again choose the case where the gradients at the upstream and downstream boundaries are zero so that the viscous flux there is also zero. There exists an unsteady solution where the flow variables at the upstream and downstream boundaries are constant, again as in the steady case. The integrated equation is now

$$\begin{aligned} \frac{\mathrm{d}}{\mathrm{d}t}\int U\,\mathrm{d}x &= -[(F_E)_{\text{downstream}} - (F_E)_{\text{upstream}}] \\ &= \text{const} \end{aligned} \tag{8}$$

What happens to this equation when time is advanced from 0 to T? The time derivative can now be written in terms of the solution at time 0 and T:

$$\begin{aligned} &\int U(x, T)\,\mathrm{d}x - \int U(x, 0)\,\mathrm{d}x \\ &\quad = -T[(F_E)_{\text{downstream}} - (F_E)_{\text{upstream}}] \end{aligned} \tag{9}$$

The only possible solution to this equation is a constant moving flowfield that is, in fact, the steady-state flowfield moving at some constant velocity. In the time from 0 to T, the steady flowfield has moved some distance X, as shown in Fig. 1. Putting this information together gives

$$\dot{x}_s(U_{\text{downstream}} - U_{\text{upstream}}) = [(F_E)_{\text{downstream}} - (F_E)_{\text{upstream}}] \tag{10}$$

which in the notation defined earlier for the jump across the shock is

$$[\![F_E - \dot{x}_s U]\!] = 0 \tag{11}$$

As in the steady case, the level of viscosity only plays a role in stretching the shock region, and so it is possible to use artificial viscosity to computationally model the moving shock.

Shock Motion in a Variable Area Duct

In the previous section, several issues concerning the true one-dimensional duct, or shock tube, problem were investigated. In particular, it was found that the viscosity only plays the role of scaling the viscous shock region in both the steady and unsteady cases. But to more accurately model the real problems in which shocks are encountered, the case where the flow upstream and downstream of the shock varies will be discussed. The shock position and strength will now be clearly dependent on the viscosity because the gradients away from the shock region are no longer zero. But how strong is this

dependence? Is it part of a higher order effect that can be neglected? These are the questions that will now be answered.

To model this variable area duct, a new variable h that represents the height of the duct will be added to Eq. (1). The duct geometry will be given as part of the problem definition. The flow variables represented in the vector U are constant across the duct but vary along the duct. This duct problem would more accurately be described as a stream tube since the walls of the duct are treated as slip surfaces. The governing equation becomes

$$\frac{\partial(Uh)}{\partial t}+\frac{\partial(F_E h)}{\partial x}+\frac{\partial(F_V h)}{\partial x}-P\frac{\partial h}{\partial x}=0 \tag{12}$$

where, along with the vectors in Eq. (2), P has been defined as

$$P=\begin{bmatrix}0\\ p\\ 0\end{bmatrix} \tag{13}$$

Let a transonic region of the flowfield be divided into three subregions: the region upstream of the shock, the region around the shock, and the region downstream of the shock. The state vector in each of these regions will be called U_U, U_V, and U_D, respectively. The flow will be unsteady, and so the shock will move. Its location is again marked by x_s, which is now a function of time. Each of these regions is shown in Fig. 2. There exists an overlap region between the viscous region and the upstream and downstream solutions indicated by the dashed lines, which will be mentioned later. For now, let each region be considered in turn.

First consider the regions away from the shock represented by U_U and U_D. It is well accepted that viscous effects are negligible in these regions, as can be shown by a simple scaling argument. This argument will be applied to show that the difference between the steady solution and the unsteady solution in this region is governed by the Euler fluxes. Let the difference in the velocity u from the steady state go as $\tilde{U}$ and vary over a length L, a characteristic length scale for the geometry. The scale of the unsteadiness that is imposed at the boundaries is given by ω. The steady convection speed is $\bar{c}$, and the kinematic viscosity ν is μ/ρ. Given these parameters, each term of the equation is scaled:

$$\begin{array}{ccccccc}
\dfrac{\partial(Uh)}{\partial t} & + & \dfrac{\partial(F_E h)}{\partial x} & + & \dfrac{\partial(F_V h)}{\partial x} & - & P\dfrac{\partial h}{\partial x} \\
\downarrow & & \downarrow & & \downarrow & & \downarrow \\
\tilde{U}h\omega = & & \bar{c}\dfrac{\tilde{U}h}{L} & & \nu\dfrac{\tilde{U}h}{L^2} = & & \bar{c}\dfrac{\tilde{U}h}{L} \\
k\left(\bar{c}\dfrac{\tilde{U}h}{L}\right) & & & & \dfrac{1}{Re}\left(\bar{c}\dfrac{\tilde{U}h}{L}\right) & &
\end{array} \tag{14}$$

For reduced frequency ($k=\omega L/\bar{c}$) of order 1 (which is the region of interest in turbomachinery), all but the third term balance. This is actually true for $k \ll \mathcal{O}(Re)$. As in the steady equation, for high Reynolds number the third term is much smaller than the other terms. As stated earlier, it is clear that, to leading order, U_U and U_D are represented by the Euler solution, where the viscous term is neglected in both the steady and the unsteady solution. This is similar to the shock tube problem where the flow outside the shock region is inviscid.

Next consider the shock region represented by U_V. Again, only the unsteady solution will be considered. Since in the unsteady flowfield the shock will move, the frame of reference is changed to one moving with the shock, so that the new spatial variable is $X=x-x_s(t)$. The shock velocity is given by the time rate of change of x_s. To change frames of reference, the time derivative $(\partial/\partial t)$ is replaced by $(\partial/\partial t)-\dot{x}_s(\partial/\partial X)$, and the spatial derivative $(\partial/\partial x)$ is replaced by $(\partial/\partial X)$. Again, let the change in u from the steady state go as $\tilde{U}$, which now varies over the length δ, the shock width. The shock moves some distance $\tilde{x}_s$ from its steady location. The scale of the unsteadiness is given by the same ω as before, as is the kinematic viscosity ν. The steady convection speed $\bar{c}$ is also the same. The changes from steady state of each term of the governing equations can be scaled:

$$\begin{array}{ccccccccc}
\dfrac{\partial(Uh)}{\partial t} & - & \dot{x}_s\dfrac{\partial(Uh)}{\partial X} & + & \dfrac{\partial(F_E h)}{\partial X} & + & \dfrac{\partial(F_V h)}{\partial X} & - & P\dfrac{\partial h}{\partial X} & = 0 \\
\downarrow & & \downarrow & & \downarrow & & \downarrow & & \downarrow & \\
\tilde{U}h\omega = & & \omega\tilde{x}_s\dfrac{\tilde{U}h}{\delta} & & \bar{c}\dfrac{\tilde{U}h}{\delta} = \dfrac{L}{\delta}\left(\bar{c}\dfrac{\tilde{U}h}{L}\right) & & \nu\dfrac{\tilde{U}h}{\delta^2} = \left(\dfrac{L}{\delta}\dfrac{1}{Re}\right)\dfrac{L}{\delta}\left(\bar{c}\dfrac{\tilde{U}h}{L}\right) & & \bar{c}\dfrac{\tilde{U}h}{\delta} = \dfrac{L}{\delta}\left(\bar{c}\dfrac{\tilde{U}h}{L}\right) & \\
 & & & & = Re\left(\bar{c}\dfrac{\tilde{U}h}{L}\right) & & = Re\left(\bar{c}\dfrac{\tilde{U}h}{L}\right) & & = Re\left(\bar{c}\dfrac{\tilde{U}h}{L}\right) &
\end{array} \tag{15}$$

The shock is defined by the region where the last three terms balance, which implies that $\delta/L=\mathcal{O}(Re^{-1})$. Since ω and $\bar{c}$ are the same as before, but given $\delta \ll L$, the first term that describes the unsteadiness is much smaller than the last three and can be neglected. From this it is argued that the leading-order term of the shock shape U_V is quasisteady. At any instant in time, the shape of the shock is a steady function given the boundary conditions upstream and downstream of this region.

Again, like the shock tube problem, a coordinate transformation can be made such that $\xi=X/\mu_{\text{ref}}$, which is merely a stretching of the shock region. This transformation renders the equations unchanged except that the parameter μ is replaced by the nondimensional μ/μ_{ref}. This again implies that the shock width is a function of the viscosity, but the shape of the shock is not.

What has been learned is that, as with the steady flowfield, the region away from the shock is not governed by the full Navier-Stokes equations but by the inviscid Euler equations.

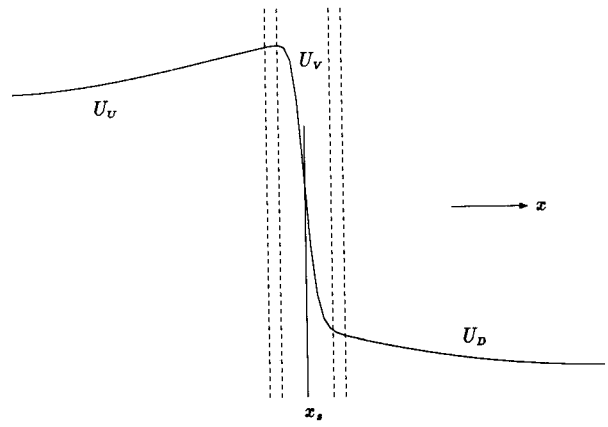

Fig. 2 Regions around a shock for analysis.

In the shock region the shape of the shock is governed by the boundary conditions on the shock region, but the viscosity only governs the width. Other than the unsteady boundary conditions, the shock region has no temporal dependence but is a quasisteady function of the upstream and downstream solutions.

It can be shown that the terms that are neglected in the preceding analysis are in error by a contribution of $\mathcal{O}(1/Re)$, which is negligibly small; hence, in each region, the leading-order solutions are quite accurate. Asymptotic matching between the regions provides a smooth transition in the intermediate regions shown in Fig. 2.[4,9]

For many calculations, it is important to know the unsteady forces on the moving blade due to the unsteady fluid motion, for example, to determine if the fluid causes a flutter mode to amplify or decay. The flow will be modeled as a steady flow with an unsteady perturbation so that in one dimension the unsteady state vector becomes $U(x, t) = \bar{U}(x) + \tilde{U}(x, t)$. Does the viscous flowfield just discussed conform to this assumption? This question will be answered by determining if the lift perturbation $\tilde{\ell}$ in the shock region is linear with the forcing perturbation when the flow away from the shock is in the linear regime.

The lift perturbation is the integral of the unsteady pressure perturbation given by $\tilde{\ell} = \int \tilde{p}\, dx$. In Fig. 3, four possibilities for the lift perturbation with a perturbation shock movement $\tilde{x}_s(t)$ are shown. Each possibility represents different levels of unsteady shock motion. The most important length scale with which to compare the shock motion is the width of the shock; therefore this is the length scale that defines the four regions. In each case the question of linearity between the lift perturbation and the shock movement is discussed.

$\tilde{x}_s \ll \delta$: In this region the shock movement is much smaller than the width of the shock. An example is given in the first case of Fig. 4. The shock moves, but the strength of the shock remains nearly constant. To leading order this is just the translation of the shock, and so the lift perturbation due to the movement of the shock is just the decrease in pressure across the shock times the movement of the shock. The lift perturbation is clearly linear with the shock movement where the linearity constant is the jump in pressure. This case is what would be considered "linear viscous," since the effect of unsteadiness is small and the effect of viscosity is large, and represents a solution of the linear Navier-Stokes equations.

$\delta \ll \tilde{x}_s \ll L$: In this region the lift perturbation can also be shown to be linear. This is the third case in Fig. 4. The change in the shape of the shock is negligible compared with the area over which the shock traveled, and so the lift perturbation due to the movement of the shock is again the decrease in pressure across the shock times the movement of the shock, the same linear function as was found before. The lift perturbation from influences other than the shock movement is linear by definition since the rest of the flowfield is linear. This can essentially be considered as the inviscid limit for the shock; it will be called "linear inviscid" and represents a solution of the linear Euler equations.

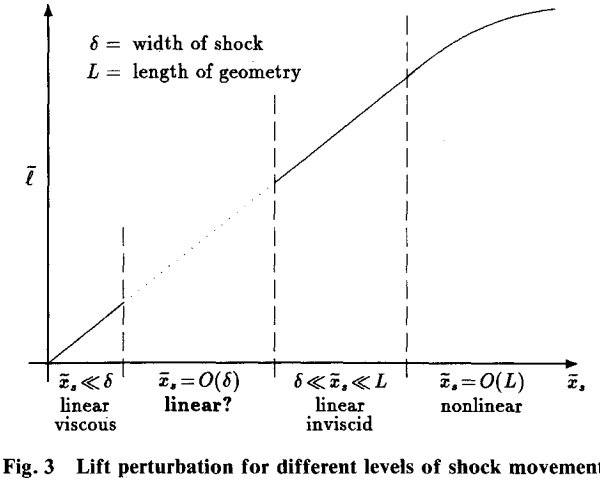

Fig. 3 Lift perturbation for different levels of shock movement.

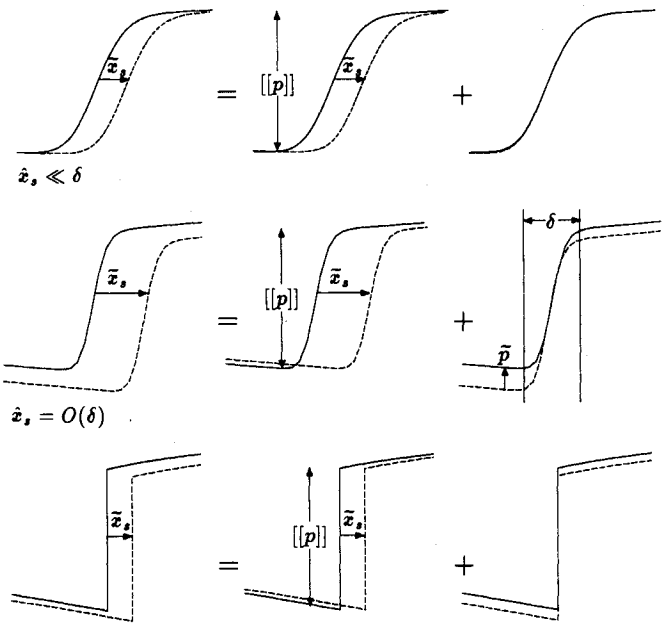

Fig. 4 Shock movement for various relative levels of shock width and shock motion. To leading order the change in integrated lift $\tilde{\ell} = -[\![p]\!]\tilde{x}_s$ in all cases.

$\tilde{x}_s = \mathcal{O}(L)$: When the shock movement is on the same order as the length scale of the geometry, the rest of the flowfield will probably be in the nonlinear regime, and so in this region the lift perturbation is not linear with the shock movement.

What remains is the region where the shock movement is of the same order as the shock width [$\tilde{x}_s = \mathcal{O}(\delta)$]. This case is more complicated than the previous three cases and makes use of the scaling analysis presented earlier in this section. In particular the information from this scaling analysis that will be used here is the following:

1) The viscosity only determines the scaling of the shock shape.

2) The shock shape itself is a quasisteady function of $U_U(x_s)$ and $U_D(x_s)$, the Euler solution at the shock.

As shown in the middle case of Fig. 4, when the shock moves some $\tilde{x}_s$, the contribution to the lift can be divided into two parts: one due to the movement of the shock and the other due to the change in strength of the shock. The contribution to the lift perturbation from the shock movement is as before, the decrease in pressure across the shock times the shock movement. Where before the contribution from the amplitude change of the shock could be easily neglected, here it cannot be dismissed so easily. Since, from statement 1, the shock shape is a quasisteady function of the flow upstream and downstream of the shock, and the steady shock shapes are similar; the two unsteady shock shapes in this figure are also similar. Therefore, the contribution from the amplitude change is approximately equal to the pressure perturbation on the upstream or downstream sides of the shock times the width of the shock. This can most easily be seen by examining the contribution to the amplitude change in Fig. 4. Away from the shock, the pressure perturbations are small as is the shock width. Since both δ and $\tilde{p}$ are small compared with $[\![p]\!]$, this is a higher order effect compared with the contribution from the movement of the shock. This case really draws the linear viscous and linear inviscid cases together. Considering the limit of this case where the viscosity decreases to zero, or $\delta \to 0$, the width of the shock decreases and the linear inviscid case is reached. In the limit as unsteadiness goes to zero, or $\tilde{p} \to 0$, the

linear viscous case is reached. The conclusion is that the unsteady lift of a transonic flow has to leading order a lift distribution that is linear in the forcing perturbation, and the linear function is the same as for the two previous cases, $\tilde{\ell} = -[\![p]\!]\tilde{x}_s$. As long as the portion of the flowfield away from the shock is in the linear regime, the shock portion will be as well. Therefore, if either a linear viscous solution from the linear Navier-Stokes equations or a linear inviscid solution from the linear Euler equations is found, due to linearity the solution in the intermediate region is known as well.

As mentioned in the shock tube problem, it has become common practice to model a flowfield computationally with the Euler equations and use an artificial viscosity to "capture" the shock since the location and movement of the shock are independent of the viscosity, which only governs the width of the shock profile. Since the shock is so heavily smeared, for a small, unsteady perturbation of the flowfield, shock capturing with the linear Euler equations is similar to the linear viscous case presented earlier, where the movement of the shock is much smaller than the width of the shock. When shock fitting is used, the shock has no thickness, and so shock fitting is similar to the linear inviscid case. Either of these methods can be used to find the solution to the unsteady transonic flowfield. The important point is that whether shock fitting or capturing is used, there is still the same linear relationship between the shock motion $\tilde{x}_s$ and the lift perturbation $\tilde{\ell}$. This linear relationship makes these computational methods viable.

Computational Issues in Modeling the Euler Equations

The previous section looked at the analytical issues associated with a moving shock, emphasizing the need to understand the flowfield before a computational model can be developed. In this section, computational issues will be addressed to ensure that the numerical solution is consistent with this analysis. Again, the discussion starts with the constant area duct since it provides a simple model of a flowfield in which the shock motion can be examined. Next, the issues that were found to be important in the constant area duct problem will be investigated in a variable area duct problem.

Constant Area Duct

When studying the analytical solution to the shock tube problem, we found that, for both the steady and the unsteady solutions, the viscosity only plays the role in the scaling of the shock region and not in the location or strength of the shock. Here, this knowledge will be used to discuss the modeling of the shock using artificial viscosity.

The computational methods considered here will store the flow variables at discrete nodes and use linear interpolation to find the values between the nodes. Aside from the usual concerns associated with numerical schemes, such as stability or accuracy, there are concerns in this problem associated with the shock region. If the shock is modeled as a highly stretched viscous region, the shape of the shock will still only be captured in a few cells. As a shock moves, the location of the shock in the discrete approximation lands at a different place with respect to the computational nodes. By only knowing the solution at the nodes, the discrete shape of the moving shock will be different depending on its location, as shown in Fig. 5. What kind of error does this cause? Does the error due to the changing shock shape diminish in the integral of the quantity? The integrated solution is of interest since the integrated pressure represents the force on the surface and would correspond to lift or drag in a two-dimensional application. It is also the integrated quantities that provide the linearity discussed in the previous section.

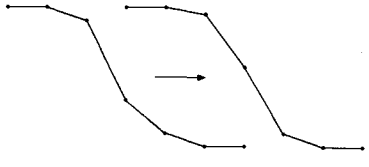

Fig. 5 Change in discrete shock shape as a shock moves.

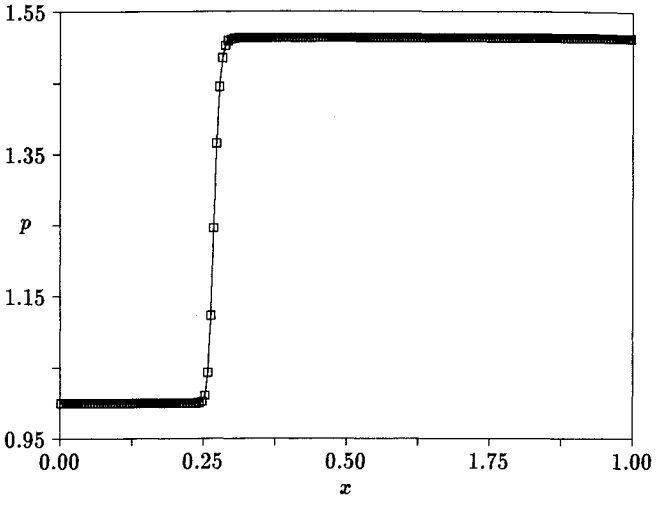

Fig. 6 Pressure for relative inlet Mach number 1.2 shock with shock speed 0.1 for second difference artificial viscosity.

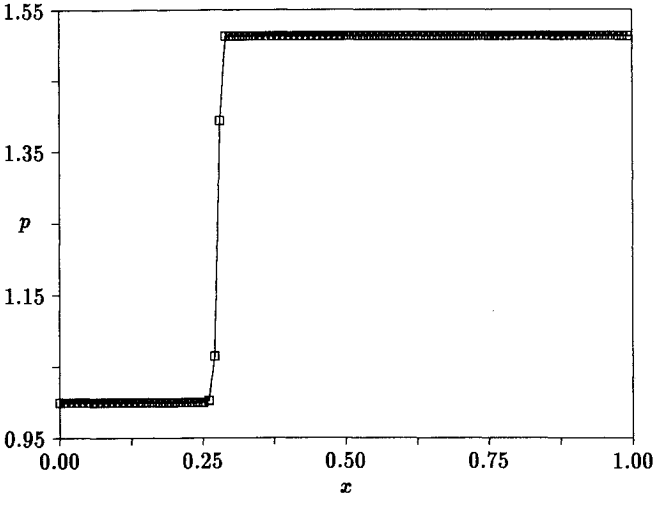

Fig. 7 Pressure for relative inlet Mach number 1.2 shock with shock speed 0.1 for flux vector split scheme.

The actual computational schemes that were used in this study will not be discussed here since they represent standard formulations that are well known in the literature. Both schemes model time integration using a four-step Runge-Kutta method.[10] Two means of computing the flux residual with different methods of shock capturing are used: a standard second difference artificial viscosity[10] and a flux vector split method.[11] One important point that must be made about these schemes is that they are conservative, or in other words they accurately model Eq. (8) computationally.

Figure 6 shows a representative shock shape for an artificial viscosity scheme. Notice that the shock region covers about eight cells in this case and produces a smooth transition between the upstream and downstream states. The representative shock shape for the flux vector split scheme is shown in Fig. 7. The flux vector split scheme produces a much crisper shock that only contains two nodes.

These numerical schemes are conservative, and so the overall solution is guaranteed to follow the exact solution since it is the boundary conditions that drive this overall solution. But what is the effect of changing shock shape due to discretization as the shock moves? If the discrete shock is smooth

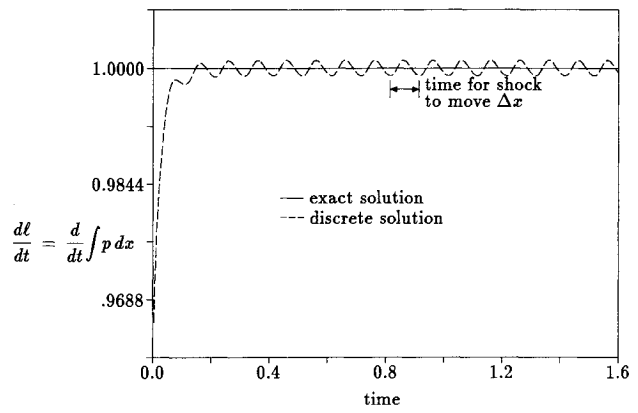

Fig. 8 Time rate of change of integrated pressure for relative inlet Mach number 1.2 shock with shock speed 0.1 for the flux vector split scheme.

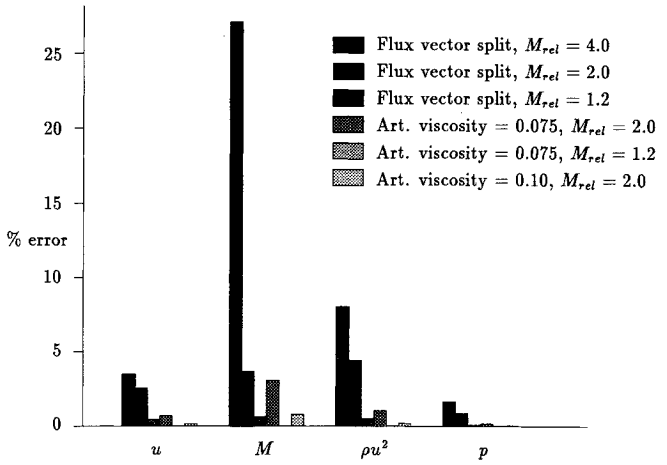

Fig. 9 For various schemes, the percent error in $(d/dt)\int(*)\,dx$ from the exact solution for the quantities u, M, ρu^2, and p.

enough, then this effect should be small because the shock shape is very well resolved regardless of its location relative to the grid. Using artificial viscosity, the shock is smeared out and keeps a similar profile from one iteration to the next. The scheme that produces the crispest shocks is flux vector splitting, which forces only two points to be in the shock and therefore has a more radically changing shock shape. This scheme should have a larger error due to discretization and in fact represents a worst case for shock-capturing schemes.

To quantify the effects of discretization on the solution, the results are presented as the difference in the integral over the whole domain from one time step to the next. The shock tube problem has an exact solution given in Eq. (8), which is only a function of the boundary values, to which the discrete value can be compared. For the conserved quantities in the state vector ρ, ρu, and ρE, the difference in the integral should be a constant in the computational results by the definition of conservation. Any other quantities may waiver about the exact solution but in the long run will track with the exact solution since they are a function of these conserved quantities. As an example, the computational rate of change in integrated pressure normalized by the exact solution is shown in Fig. 8 as a function of time for the flux vector split scheme. This is the same case for which the shock profile is shown in Fig. 7. For small time, the shock shape is settling into its natural shape. As time progresses, the function takes the shape of a periodic oscillation about the exact solution. The period of the oscillation is the time for the shock to move one computational cell. Roberts[12] found that this error can cause entropy waves to appear in the solution away from the shock.

To illustrate the effects of the changing shock shape, both schemes were run for a range of Mach numbers. The rate of change of the integral over the domain $[(d/dt)\int(*)\,dx]$ was found for several quantities. The effect of shock speed and Courant-Friedrichs-Lewy (CFL) number were investigated, but the results were found to have a weak dependence on these parameters. The percent deviation from the exact solution, or error, as shown in Fig. 8 was then computed and is shown in Fig. 9. The conserved quantities, ρ, ρu, and ρE, produce no error. It can be seen that when artificial viscosity is used, the shape of the shock is better preserved from one iteration to the next than for the flux vector split schemes, and so the magnitude of the error is reduced. With the artificial viscosity scheme, as the coefficient is increased, there are more nodes in the shock, and again the shape of the shock is better preserved so that the error is reduced. As the Mach number increases, the magnitude of the jump over the shock increases, and the error likewise increases. In most cases the error is quite small, particularly for the pressure integral.

The small error in the pressure integral is of particular interest since the lift, more than any other integral value, is of interest from a fluid dynamics point of view. This behavior can be explained by looking at the relationship between the pressure and the conserved quantity ρE, total energy, which is conserved. The time rate of change of integrated pressure can be written as

$$\frac{d}{dt}\int p\,dx = (\gamma - 1)\left[\frac{d}{dt}\int \rho E\,dx - \frac{1}{2}\frac{d}{dt}\int \rho u^2\,dx\right] \tag{16}$$

For the case of a zero-width, inviscid shock, this is another statement of the shock jump relations:

$$[\![p]\!] = (\gamma - 1)([\![\rho E]\!] - \tfrac{1}{2}[\![\rho u^2]\!]) \tag{17}$$

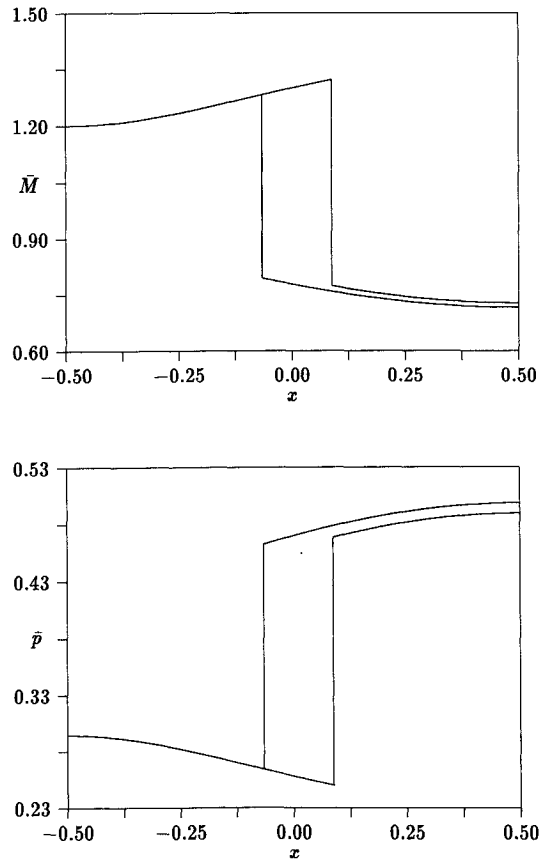

Fig. 10 Mach number and pressure distribution for two flow solutions defined by two different exit pressures that form an envelope for solutions with exit pressures between these bounds.

Using the shock jump relation in Eq. (11), one can easily show that

$$[\![\rho u^2 + p - \dot{x}_s \rho u]\!] = 0$$

$$[\![p]\!] = -[\![\rho u^2]\!] + \dot{x}_s [\![\rho u]\!]$$

$$= -[\![\rho u^2]\!] + \dot{x}_s^2 [\![\rho]\!]$$

When $\gamma = 1.4$ and the shock speed is small, the second term in Eq. (17) contributes an amount that is only 20% of the total integral in pressure,

$$\frac{-\frac{1}{2}(\gamma-1)[\![\rho u^2]\!]}{[\![p]\!]} = \frac{1}{2}(\gamma-1) - \dot{x}_s^2 \frac{[\![\rho]\!]}{[\![p]\!]} \approx 0.20 \qquad (18)$$

so that the conserved quantity ρE contributes 80% to the rate of change of the integral. Since this larger term does not contribute to the errors due to conservation, all of the error comes from the much smaller $\frac{1}{2}\rho u^2$ contribution.

Variable Area Duct

In the analysis presented earlier, it was found that the relationship between the integrated pressure, or lift, and the location of the shock was linear. An important point in this analysis is that analytically the shock shape would remain similar as it moved. Here, the effects of discretization on this result will be examined. In essence, the results from the shock tube problem are directly applicable to the variable area duct (since it is the effect of changing shock shape that is in question), but to justify this statement an example will be presented.

The problem will be a quasisteady, quasi-one-dimensional duct problem with variable exit pressure. The nonlinear problem will be examined, although the question of whether this flowfield is linear will be at the heart of the discussion. The focus will be on the definition of linearity. Here the relationship between the lift and the exit pressure for a transonic duct will be examined both analytically and computationally.

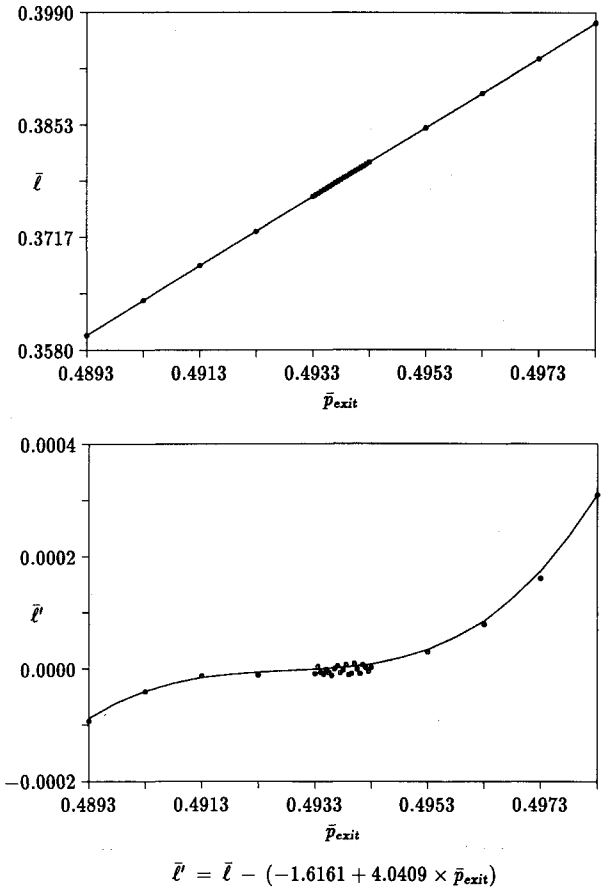

Fig. 11 Steady lift as a function of exit pressure for the envelope defined by solutions shown in Fig. 10 for exact solutions and computational solutions, and this function after the linear terms are removed. The computational solution is only sampled at the symbols.

In Fig. 10, two similar transonic flow solutions are shown for two exit pressures, $p_{exit} = 0.4893$ and 0.4983. Since the steady, variable area duct has an exact solution, this is essentially what is plotted here. All that was varied to find these solutions was the exit pressure. A solution with an exit pressure between these two bounds would fall somewhere between these solutions, which in essence form an envelope for a whole set of solutions.

In Fig. 11, the steady lift for this envelope of solutions is plotted as a function of exit pressure in this envelope. The set of symbols in this figure represent several computational solutions, where each symbol represents a separate steady calculation. The computational scheme uses second difference artificial viscosity. More samples were taken in the center of the domain, illustrated by the greater clustering of the symbols. Notice that the relationship between these variables is nearly linear. When a linear function is subtracted from the steady lift $\bar{\ell}$ to create a new variable $\bar{\ell}'$, it can be seen that the relationship is not exactly linear but contains some slight nonlinearity. This is the result that would be expected given the analysis for a variable area duct. The symbols in this figure deviate from the exact solution, due to the changing shock shape that was seen in the shock tube problem. This pattern of deviation from the exact solution will continue through the whole domain. The error due to the changing shock shape in this solution is approximately 0.04%. This computational error represents such a small deviation from the linearity that, to leading order, linearity can be assumed for the computational solution as well as the exact solution.

Again, the effect of changing shock shape in the variable area duct is the same effect illustrated with the constant area duct shock tube. The errors associated with this changing shock shape are of the same magnitude as the errors found for similar shock tube problems.

Conclusions

This article first looked at the analytical issues associated with unsteady shocks. It was found that, for both the constant and variable area ducts, the role of viscosity in the shock region was to scale the width of the shock. In the unsteady shock tube problem, the shock motion is merely a translation of the shock region. In the shock region of a variable area duct problem, this is true in the linear viscous and linear inviscid solution regimes. The unsteadiness in the linear viscous solution is actually the solution to the linearized Navier-Stokes equations, whereas the linear inviscid solution corresponds to the linearized Euler equations. Because of the linear nature of integrated quantities, of the solution, such as lift, it is necessary to find only the linear viscous or linear inviscid solution to find a solution in the intermediate region.

When computing a solution to the linearized equations with shock capturing, what is actually being found is something similar to the linear viscous solution. The shock region has a width on the order of a few computational cells, but this is analogous to increasing the viscosity, which plays the role of a scale factor. Shock fitting represents the linear Euler solution. The analysis presented here demonstrates the equivalence of these two approaches. Next, the question of discretization effects was examined. The important issue was the changing shape of a discretized moving shock. The discrete shock was looked at in detail with a constant area duct, and it was found that these errors are small, particularly for the integrated pressure, or lift, which is the integrated quantity of interest for the problems in question. This conclusion carries over to the variable area duct problem as well.

Linear perturbation methods are significantly less expensive than full nonlinear unsteady calculations. This and the in-

creased flexibility of shock-capturing schemes have prompted the examination of the use of shock capturing with linear schemes. The arguments given here showed the viability of these schemes and have led the authors and others to develop computational methods based on the linear Euler equations with shock capturing.[4,6,7,9]

References

[1]Whitehead, D. S., "The Calculation of Steady and Unsteady Transonic Flow in Cascades," Cambridge Univ. Engineering Dept., Technical Rept. CUED/A-Turbo/TR 118, Cambridge, England, UK, Feb. 1982.

[2]Verdon, J. M., and Casper, J. R., "A Linearized Unsteady Aerodynamic Analysis for Transonic Flows," *Journal of Fluid Mechanics,* Vol. 149, 1984, pp. 403–429.

[3]Hall, K. C., and Crawley, E. F., "Calculation of Unsteady Flows in Turbomachinery Using the Linearized Euler Equations," *AIAA Journal,* Vol. 27, No. 6, 1989, pp. 777–787.

[4]Lindquist, D. R., and Giles, M. B., "On the Validity of Linearized Unsteady Euler Equations with Shock Capturing," AIAA Paper 91-1598, June 1991.

[5]Kahl, G., and Klose, A., "Time Linearized Euler Calculations for Unsteady Quasi-3D Cascade Flows," *Sixth International Symposium on Unsteady Aerodynamics, Aeroacoustics and Aeroelasticity of Turbomachines and Propellers* (Univ. of Notre Dame, Notre Dame, IN, 1991), Springer-Verlag, New York, 1993.

[6]Holmes, D. G., and Chuang, H. A., "Two Dimensional Linearized Harmonic Euler Flow Analysis for Flutter and Forced Response," *Sixth International Symposium on Unsteady Aerodynamics, Aeroacoustics and Aeroelasticity of Turbomachines and Propellers* (Univ. of Notre Dame, Notre Dame, IN, 1991), Springer-Verlag, New York, 1993.

[7]Giles, M. B., "A Framework for Multi-Stage Unsteady Flow Calculations," *Sixth International Symposium on Unsteady Aerodynamics, Aeroacoustics and Aeroelasticity of Turbomachines and Propellers* (Univ. of Notre Dame, Notre Dame, IN, 1991), Springer-Verlag, New York, 1993.

[8]Hall, K. C., "A Linearized Euler Analysis of Unsteady Flows in Turbomachinery," Ph.D. Dissertation, Dept. of Aeronautics and Astronautics, Massachusetts Inst. of Technology, Cambridge, MA, May 1987.

[9]Lindquist, D. R., "Computation of Unsteady Transonic Flowfields Using Shock Capturing and the Linear Perturbation Euler Equations," Ph.D. Dissertation, Dept. of Aeronautics and Astronautics, Massachusetts Inst. of Technology, Cambridge, MA, Dec. 1991.

[10]Jameson, A., Schmidt, W., and Turkel, E., "Numerical Solutions of the Euler Equations by a Finite Volume Method Using Runge-Kutta Time Stepping Schemes," AIAA Paper 81-1259, June 1981.

[11]Van Leer, B., "Flux-Vector Splitting for the Euler Equations," Inst. for Computer Applications in Science and Engineering, TR 82-30, Hampton, VA, Sept. 1982; also *Lecture Notes in Physics,* Vol. 170, 1982, pp. 507–512.

[12]Roberts, T. W., "The Behavior of Flux Difference Splitting Schemes Near Slowly Moving Shock Waves," *Numerical Methods for Fluid Dynamics III,* edited by K. W. Morton and M. J. Baines, Oxford Science Publications, Oxford, England, UK, March 1988, pp. 442–448.